



## Endonuclease-responsive aptamer-functionalized hydrogel coating for sequential catch and release of cancer cells

Shihui Li<sup>a,1</sup>, Niancao Chen<sup>a,1</sup>, Zhaoyang Zhang<sup>b,c</sup>, Yong Wang<sup>a,b,\*</sup>

<sup>a</sup> Program of Biomedical Engineering, School of Engineering, University of Connecticut, Storrs, CT 06269-3222, USA

<sup>b</sup> Department of Chemical, Materials & Biomolecular Engineering, University of Connecticut, Storrs, CT 06269-3222, USA

<sup>c</sup> National Institutes for Food and Drug Control, Beijing 100050, China

### ARTICLE INFO

#### Article history:

Received 15 August 2012

Accepted 17 September 2012

Available online 17 October 2012

#### Keywords:

Hydrogel

Affinity

Interface

Enzyme

Cell adhesion

Biocompatibility

### ABSTRACT

Rare circulating tumor cells are a promising biomarker for the detection, diagnosis, and monitoring of cancer. However, it remains a challenge to develop biomedical devices for specific catch and nondestructive release of circulating tumor cells. The purpose of this study was to explore a unique system for cell catch and release by using aptamer-functionalized hydrogels and restriction endonucleases. The results show that the hydrogel coating was highly resistant to nonspecific cell binding with  $\sim 5\text{--}15$  cells/mm<sup>2</sup> on the hydrogel surface. In contrast, under the same condition, the aptamer-functionalized hydrogel coating could catch target cancer cells with a density over 1000 cells/mm<sup>2</sup>. When the hydrogel coating was further treated with the restriction endonucleases, the bound cells were released from the hydrogel coating because of the endonuclease-mediated sequence-specific hydrolysis of the aptamer sequences. The release efficiency reached  $\sim 99\%$ . Importantly,  $\sim 98\%$  of the released cells maintained viability. Taken together, this study demonstrates that it is promising to apply endonuclease-responsive aptamer-functionalized hydrogels as a coating material to develop medical devices for specific catch and nondestructive release of rare circulating tumor cells.

© 2012 Elsevier Ltd. All rights reserved.

### 1. Introduction

Circulating tumor cells in blood are a promising biomarker to determine the stage of a tumor and to guide the design of an appropriate therapeutic protocol [1–5]. However, these cells have a very small population. In general, there are less than 10 circulating tumor cells in 1 mL blood of a cancer patient whereas the same volume of blood contains approximately  $5 \times 10^9$  normal cells [3]. Therefore, a variety of methods and materials have been recently investigated for sensitive detection and accurate characterization of rare circulating tumor cells.

Tumor cells in a blood sample can in principle be detected by the quantification of specific messenger RNAs with polymerase chain reaction (PCR) [6–9]. However, presumably because of the instability of RNAs and the complex amplification procedure, the PCR-based cell analysis often leads to results with considerable variations or even false-positive results [3]. Alternatively, circulating

tumor cells can be examined directly through cytometric analysis. Because circulating tumor cells have a very small number in comparison to the entire cell population, specific cell labeling and immunomagnetic enrichment are often applied to pretreat a blood sample [10,11]. After the pretreatment, the cell mixture can be analyzed with numerous methods [3]. A commonly used method is flow cytometry [11,12]. Some clinical studies have demonstrated that flow cytometry is very sensitive and can detect a single tumor cell per  $10^7$  cells [11]. However, circulating tumor cells have been found to form clusters or aggregates that have different scatter characteristics from individual cells [3]. Thus, the need of sample pretreatment and the heterogeneous geometry of tumor cells might compromise the sensitivity of cytometric analysis.

Recently, affinity-based microfluidic systems have been extensively studied for selective separation and detection of viable circulating tumor cells from the whole blood without the need of pre-labeling or processing samples [13,14]. The examination of temporal changes in the number of circulating tumor cells has showed a reasonable correlation with the stage of disease determined by standard radiographic methods. Despite great promise, there are still two critical issues that need to be addressed. One is the specificity of cell catch because the identified circulating tumor cells exhibited approximately 50% purity [13]. The other is the

\* Corresponding author. Program of Biomedical Engineering, School of Engineering, University of Connecticut, 191 Auditorium Road, Storrs, CT 06269-3222, USA. Tel.: +1 860 486 4072; fax: +1 860 486 2959.

E-mail address: [yongwang@engr.uconn.edu](mailto:yongwang@engr.uconn.edu) (Y. Wang).

<sup>1</sup> Equally contributed.

capability to release tumor cells nondestructively after cell catch. Strong cell binding can trigger intracellular signaling cascades or even cell death [15–17], which will undoubtedly produce negative effects on the critical analysis of circulating tumor cells. Therefore, significant efforts are needed to address these two issues.

The development of an appropriate device for cell separation mainly involves the upstream design of biomolecules and coatings and the downstream optimization of device geometry and flow conditions [18–23]. This study focused on the former one, aiming to develop a system for specific catch and nondestructive release of target cells using aptamer-functionalized hydrogels as a coating material and restriction endonucleases as a cell release reagent (Fig. 1). Aptamer-functionalized hydrogels are an emerging biomaterial and have recently attracted great attention in the fields of drug delivery [24], biomimetic engineering [25], and molecular biosensing [26]. However, no attempt has been made to explore their potential for the development of medical devices for cell separation. In this study, aptamer-functionalized hydrogels were coated on a glass surface for cell type-specific catch. Numerous control surfaces were also investigated to evaluate the specificity of aptamer-functionalized hydrogels in catching target cancer cells. After the examination of cell catch, two types of restriction endonucleases were used to release cells from the hydrogel surface. Both the specificity and kinetics of cell release were studied. A cell-staining assay was also carried out to determine whether the entire procedure of cell catch and release would cause the decrease of cell viability.

## 2. Materials and methods

### 2.1. Chemical reagents

The acrylamide/bis-acrylamide solution (40% w/v; 29:1), ammonium persulfate (APS), N,N,N',N'-tetramethylethylenediamine (TEMED), phosphate buffered saline (PBS), and sodium hydroxide were obtained from Fisher Scientific (Suwanee, GA). 3-(Trimethoxysilyl) propyl methacrylate (TMSPM), the magnesium chloride solution (1.0 M), and the glucose solution (45% w/v) were purchased from Sigma–Aldrich (Louis, MO). Dulbecco's phosphate buffered saline (DPBS), bovine serum albumin (BSA), and LIVE/DEAD staining kit were all purchased from Invitrogen (Carlsbad, CA). Nucleic acid oligonucleotides (Table 1) were produced by Integrated DNA Technologies (Coralville, IA) and used directly without further purification. Restriction endonucleases *Bam*HI-HF (100,000 units/mL) and *Kpn*I-HF (100,000 units/mL) were purchased from New England Biolabs (Ipswich, MA). RPMI medium 1640 was obtained from ATCC (Manassas, VA). Fetal bovine serum (FBS, 10%) and the penicillin–streptomycin solution (100 units/mL) were purchased from Hyclone (Logan, UT). The trypsin solution (0.05% w/v) was purchased from Mediatech (Manassas, VA).

### 2.2. Preparation of silanized glass surface

Glass slides (Fisher Scientific, Suwanee, GA) were cut into small squares with a dimension of  $4 \times 4 \text{ mm}^2$ . The glass squares were sonicated in NaOH (1.0 M) for 10 min. After washed thoroughly with deionized water, the slides were treated for

5 min in a silanization solution that was prepared by diluting TMSPM (0.5 mL) in the mixture of ethanol (50 mL) and diluted glacial acetic acid (1.5 mL, 10% v/v). The silanized glass squares were washed with ethanol, dried in the air and stored in a vacuum desiccator before use.

### 2.3. Preparation of polyacrylamide hydrogel coating

Polyacrylamide hydrogels were synthesized on the silanized glass surface to produce hydrogel coatings. The pregel solution was prepared by adding TEMED (0.15  $\mu\text{L}$ , 5% v/v) into the mixture of 10% acrylamide solution (1  $\mu\text{L}$ ) containing the sequence A<sub>1A</sub> (100  $\mu\text{M}$ ) and APS (0.08  $\mu\text{L}$ , 10% w/v). Immediately after the preparation of the pregel solution, it was transferred to a supporting glass slide and covered by the silanized glass square. After 1-h polymerization, the glass square was carefully flipped off the large glass slide and rinsed thoroughly with PBS.

### 2.4. Gel electrophoresis

Complementary DNA oligonucleotides were mixed together at a molar ratio of 1:1 in PBS containing MgCl<sub>2</sub> (10 mM) and incubated at 37 °C for 1 h. Restriction enzyme (5 units) was added to cleave 1 pmol of DNA double helix at 37 °C for 0.5 h. The DNA solutions were loaded into polyacrylamide gel (10% w/v) for running electrophoresis in a Bio-Rad Mini-PROTEAN tetra cell (Hercules, CA). After electrophoresis, the polyacrylamide gel was stained with ethidium bromide and then imaged with a Bio-Rad GelDoc XR system (Hercules, CA).

### 2.5. Imaging of hydrogel coatings

Both SEM and fluorescence imaging were used to characterize hydrogel coatings. For SEM imaging, glass slides coated with affinity hydrogels were dried by lyophilization. The slides were imaged under a JEOL 6335F field emission scanning electron microscope (FESEM). For fluorescence imaging, glass slides were incubated in B<sub>1T</sub> solution (20  $\mu\text{L}$ , 5  $\mu\text{M}$  in DPBS) at 37 °C for 1 h. After thoroughly washed with DPBS, the slides were imaged under an inverted fluorescence microscope (Axiovert 40CFL, Carl Zeiss).

### 2.6. Cell culture

CCRF-CEM cells (CCL-119, human T lymphocytic leukemia cell line) and Ramos cells (Human B lymphoma cell line) were obtained from ATCC (Manassas, VA). CCRF-CEM cells were cultured in RPMI medium 1640 supplemented with 10% FBS and the 100 IU/mL penicillin–streptomycin solution. Ramos cells were cultured and maintained in RPMI medium 1640 supplemented with inactivated FBS and the penicillin–streptomycin solution. Both cells were cultured in an incubator at 37 °C in a 5% CO<sub>2</sub> atmosphere.

### 2.7. Cell catch and release

Glass squares coated with hydrogels were incubated in an aptamer solution (5  $\mu\text{M}$ ) at 37 °C to immobilize nucleic acid aptamers. After 1 h incubation, the glass squares were thoroughly washed with the binding buffer that was DPBS containing glucose (4.5 g/L), MgCl<sub>2</sub> (10 mM), and BSA (0.1% w/v). For cell catch, the glass squares were incubated in cell suspension (800  $\mu\text{L}$ ,  $5 \times 10^5$  cells/well) in a 24-well plate at 37 °C for 30 min. The unbound cells were gently removed from the coatings by shaking the plate at 90 rpm for 1 min. For cell release, the glass squares were incubated in restriction enzyme solution (80  $\mu\text{L}$ , 5 units/ $\mu\text{L}$ ) at 37 °C for 30 min. The released cells were gently rinsed off the surface by shaking the plate at 90 rpm for 10 min. The glass slides were imaged using an inverted microscope (Axiovert 40CFL,

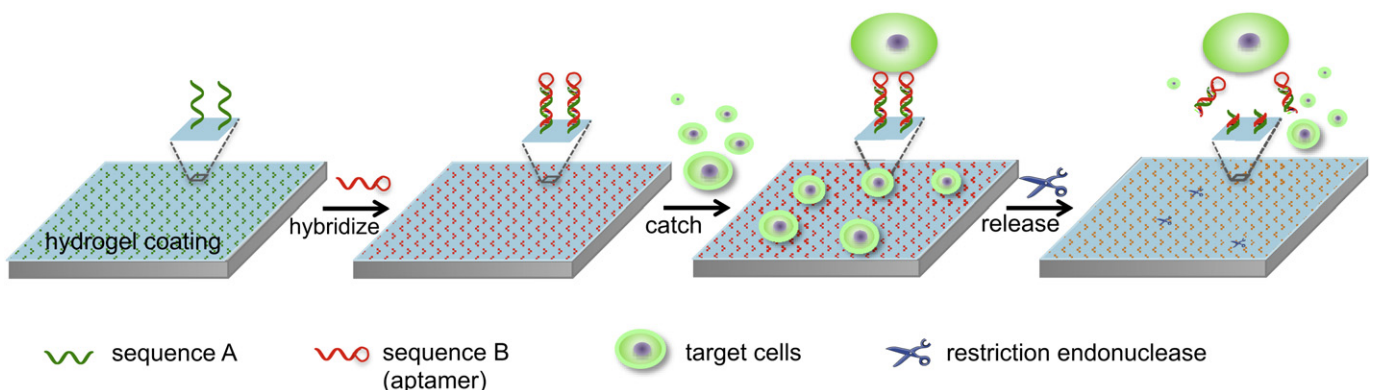


Fig. 1. Schematic of sequential cell catch and release using aptamer-functionalized hydrogel coating and restriction endonuclease.

Carl Zeiss). The cells on hydrogels were quantified using ImageJ. Three images were randomly selected for each sample. A total of three samples were used in each group.

### 2.8. Flow cytometry

Three flow cytometry experiments were run to determine the binding functionality of the hybridized aptamer, to demonstrate the endonuclease-mediated hydrolysis of the hybridized aptamer, and to test the influence of enzymatic hydrolysis on cell properties. In the first experiment,  $5 \times 10^5$  cells were incubated in mixture of  $A_{1F}$  and  $B_1$  (100  $\mu$ L) for 30 min at 4 °C. The mixture was prepared with  $A_{1F}$  (0.2  $\mu$ M) and  $B_1$  (0.1  $\mu$ M) in DPBS. After the incubation, the cells were washed with 1 mL of cold washing buffer (DPBS containing 4.5 g/L glucose and 10 mM  $MgCl_2$ ). The washed cells were immediately analyzed by the flow cytometer (BD FACSCalibur, San Jose, CA). A total of 10,000 events were counted.  $B_{1S}$  was used as control. In the second experiment, *Bam*HI (1  $\mu$ L) was added to 100  $\mu$ L of the mixture of  $A_{1F}$  and  $B_1$  and the mixture was incubated at 37 °C for 0.5 h. Afterwards, a total of  $5 \times 10^5$  CCRF-CEM cells were incubated in the *Bam*HI-treated mixture for 30 min at 4 °C, washed with cold washing buffer (1 mL), and analyzed by the flow cytometer. A total of 10,000 events were counted. In the third experiment, the cells bound to the hydrogels were treated with *Bam*HI (40 units) in an 80  $\mu$ L of binding buffer or 80  $\mu$ L of trypsin solution (0.05% w/v). FBS were added to the trypsin solution to stop cell trypsinization at the end of the release step. The released cells were labeled with the hybridized aptamer using the same protocol as described in the first flow cytometry experiment. A total of 5000 events were counted.

### 2.9. Live/dead cell staining

The released cells were stained with a mixture of calcein AM (1  $\mu$ M) and ethidium homodimer-1 (1  $\mu$ M) using the LIVE/DEAD cell staining kit. Fluorescence cell images were captured using the inverted fluorescence microscope (Axiovert 40CFL, Carl Zeiss).

## 3. Results and discussion

### 3.1. Synthesis of hydrogel coating on glass surface

Numerous methods have been studied to coat a solid surface [27]. For instance, a material can be incubated in a solution to allow for molecules to be physically adsorbed onto its surface. However, the adsorbed molecules may easily desorb under a dynamic shaking or flow condition because physical adsorption usually depends on weak hydrophobic or charge–charge interactions [27]. To stabilize a coating on a surface, the coating materials need to be conjugated to a surface via covalent bonds. In this study, we used simple, single-step free radical polymerization to synthesize a cross-linked hydrogel coating that is chemically conjugated to the glass surface. Fig. 2A shows the schematic of the synthesis of the hydrogel coating using a sandwich method. The small glass square was silanized with 3-(trimethoxysilyl)propyl methacrylate to carry methacrylate groups. When the mixture of acrylamide, bis-acrylamide, and DNA with acrydite was initiated to polymerize by APS and TEMED (Fig. 2B), the small glass square was immediately put on the liquid surface. Thus, after polymerization, the formed hydrogel was chemically conjugated to the glass square. The SEM images show that the hydrogel coating is very smooth with a thickness of  $\sim 10 \mu$ m (Fig. 2C). Importantly, when the glass square was washed and shaken in aqueous solutions, the hydrogel coating was stable on the glass surface.

### 3.2. Examination of hydrogel coating for resisting nonspecific cell binding

When a device is applied to cell separation and detection, it is important that cells do not have strong nonspecific interactions with the surface of this device. It is particularly important to separate rare circulating tumor cells from the human blood because of the overwhelmingly large number of normal cells with a diverse array of surface properties. A number of microfluidic devices have been developed for the capture of target cells based on the direct conjugation of affinity ligands to glass slides or silicon wafers [13,20–23]. Many of these devices did not exhibit the problem of nonspecific cell binding. However, other studies show that a specific coating is often necessary to avoid nonspecific binding [28–31]. This difference in literature may be attributed to the use of different techniques of surface treatment or operating conditions.

In this study, we examined nonspecific cell binding in a pseudo-static condition, in which cells were allowed to gradually precipitate to the material surface from the cell suspension. Different surfaces were studied and compared, including untreated glass surface, NaOH treated glass surface, silanized glass surface, and the hydrogel coating. The cell images show that the density of CCRF-CEM cells on the untreated glass surface, NaOH treated glass surface, and silanized glass surface were  $\sim 1100$ , 1200, and 1400 cells/ $mm^2$ , respectively (Fig. 3). In contrast, the cell density on the hydrogel coating was  $\sim 5$  cells/ $mm^2$  (Fig. 3). These results indicate that it would be important to prepare a coating to prevent nonspecific cell binding to the surface of a device, and that the hydrogel coating would be suitable for solving this non-specific binding problem. Although the polyacrylamide hydrogel was studied herein, other polymeric hydrogels (e.g., poly(ethylene glycol) (PEG), poly(vinyl alcohol), and poly(2-hydroxyethyl methacrylate)) may provide similar or better effectiveness in resisting nonspecific cell binding. In addition to the hydrogels, other materials such as PEG brush [32,33] and zwitterionic polymers [34,35] may also be used to reduce nonspecific cell binding. Moreover, the variation of numerous reaction conditions may further improve the capability of the hydrogel coating in resisting nonspecific cell binding.

### 3.3. Examination of aptamer-functionalized hydrogel coating for catching cells

After demonstrating the functionality of the polyacrylamide hydrogel in resisting nonspecific cell binding, we studied whether aptamers were capable of inducing cell type-specific binding to the polyacrylamide hydrogel. The model aptamer used in this study was originally selected from a DNA library to bind CCRF-CEM cells with Ramos cells as a negative control [36]. Its functionality has been well studied. Therefore, CCRF-CEM cells and Ramos cells were used as positive and negative cells to illustrate the concept. The aptamer (i.e., sequence B) was rationally designed to present three functional regions (Fig. 4A). The first region is the binding motif that is the

**Table 1**  
List of DNA oligonucleotides.

Name	Sequence (5'–3')
$A_1$	ATATTGTTTGTACACGGGATCCCGATTTT
$A_{1A}$	Acrydite-ATATTGTTTGTACACGGGATCCCGATTTT
$A_{1F}$	ATATTGTTTGTACACGGGATCCCGATTTT-FAM
$A_{2A}$	Acrydite-ATATTGTTTGTACAGGGTACCCCATTTT
$B_1$	TCTAACTGCTGCGCCGCGGAAAATACTGTACGGTTAGATAGTAAAAATCGGGATCCCGTGTA
$B_{1S}$	CAATGGCGTTGGGAGGACTCCGGTACTGATTACGTCAATCACAATAATCGGGATCCCGTGTA
$B_{1T}$	TCTAACTGCTGCGCCGCGGAAAATACTGTACGGTTAGATAGTAAAAATCGGGATCCCGTGTA-TAMRA
$B_2$	TCTAACTGCTGCGCCGCGGAAAATACTGTACGGTTAGATAGTAAAAATGGGGTACCCCTGTA

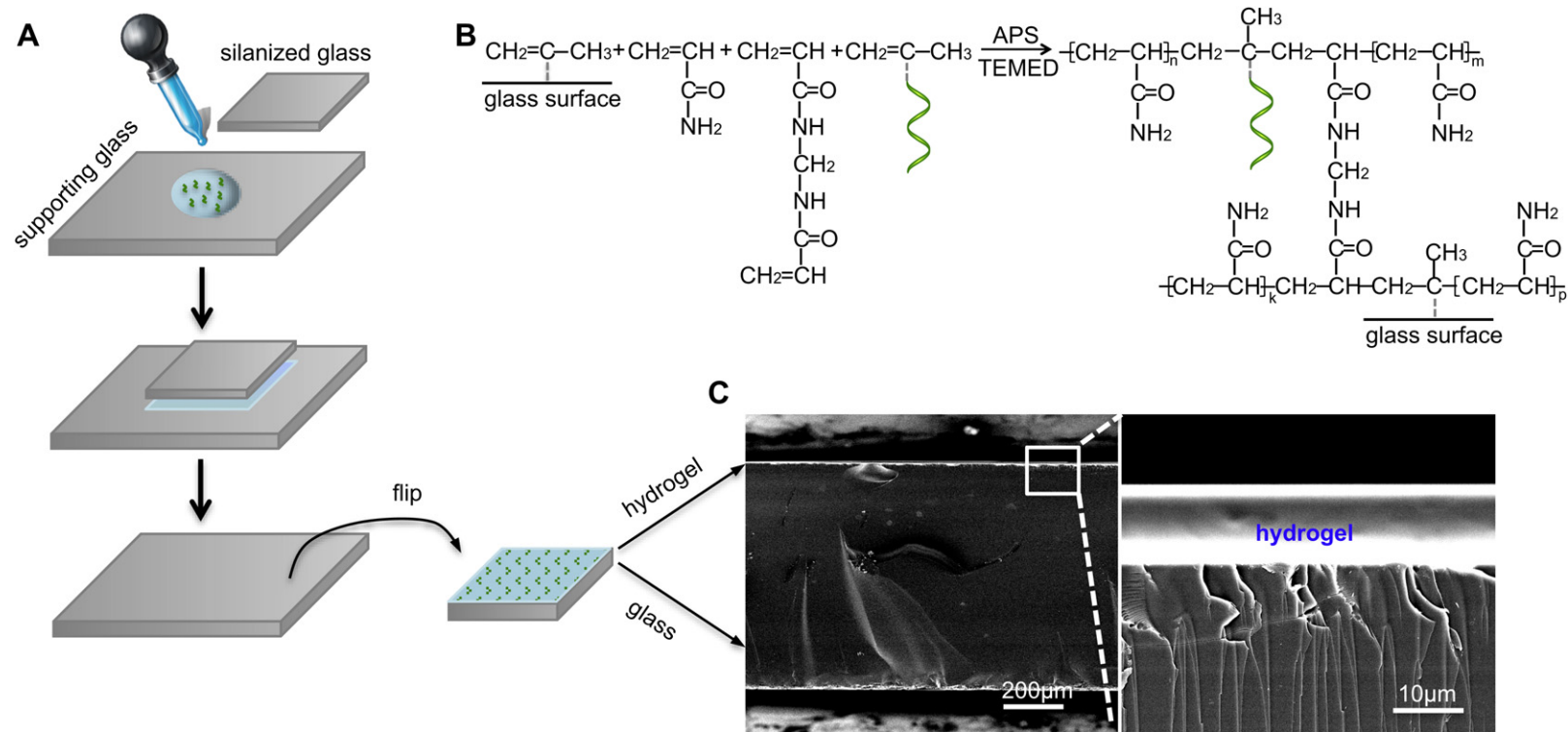


**Fig. 2.** Preparation of hydrogel coating. (A) Schematic of the sandwich method for coating a polyacrylamide hydrogel on the glass square. (B) Chemical structures and the principle of chemical reaction. (C) SEM images.

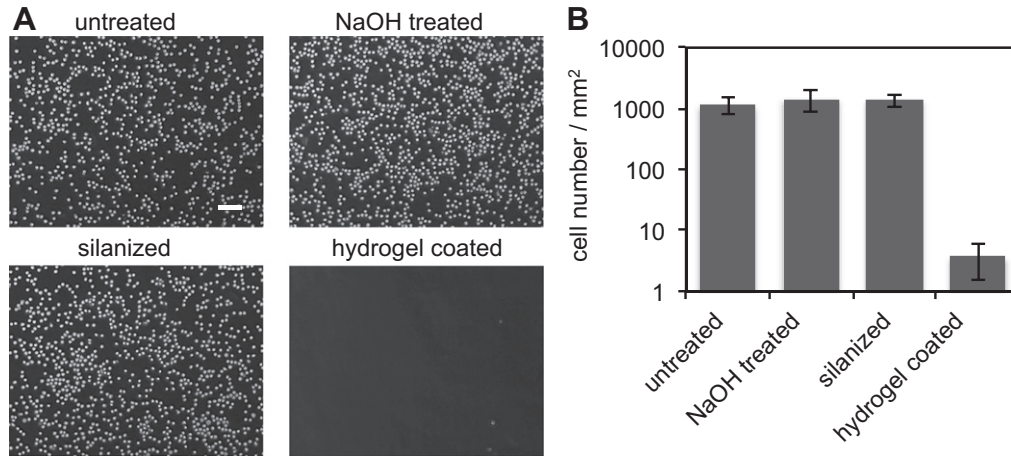


**Fig. 3.** Characterization of the functionality of the polyacrylamide hydrogel coating in resisting nonspecific cell binding. (A) Representative microscopy images of cells on different surfaces. (B) Comparison of the density of cells on different surfaces. The cell numbers were quantified with ImageJ. Scale bar: 10  $\mu\text{m}$ .

same as that of the parent aptamer. It contains a total of 40 nucleotides. The second region is a five-nucleotide linker used to increase molecular flexibility and reduce steric hindrance. The third region is a twenty-nucleotide tail used to hybridize with sequence A immobilized in the hydrogel. Importantly, this tail was specially designed with a restriction endonuclease cleavage site in the middle.

The sequences  $A_1$  and  $B_1$  can hybridize through 20 base pairs with a melting temperature higher than 60  $^{\circ}\text{C}$ . The control sequence  $B_{1S}$  can also form the same 20 base pairs with the sequence  $A_1$ . The gel electrophoretogram showed that these pairs stably hybridized in aqueous solutions (Fig. 4B). In addition to the examination of intermolecular hybridization in aqueous solutions, we also investigated the feasibility of hybridizing these sequences in the hydrogel coatings (Fig. 4C). A total of three hydrogels were synthesized. The first one was a native polyacrylamide hydrogel.

The second one was a polyacrylamide hydrogel that was prepared with a pregel solution containing sequence  $A_1$  without acrydite. Because sequence  $A_1$  did not have acrydite, it would not be able to participate in free radical polymerization. In contrary, the third one was prepared with the pregel solution containing sequence A with acrydite (*i.e.*,  $A_{1A}$ ). Thus, during the free radical polymerization, acrydite enabled the chemical incorporation of sequence A into the hydrogel network. All three hydrogel coatings were treated with sequence  $B_{1T}$  and then subjected to thorough washing. TAMRA was used to label sequence  $B_{1T}$  for clear legibility of the hybridization. The fluorescence image shows that the  $A_{1A}$  hydrogel exhibited stronger fluorescence intensity than the other two hydrogels (Fig. 4C). It demonstrates that  $A_1$  was successfully incorporated into the hydrogel, and that  $A_1$  and  $B_{1T}$  hybridized successfully in the hydrogel.

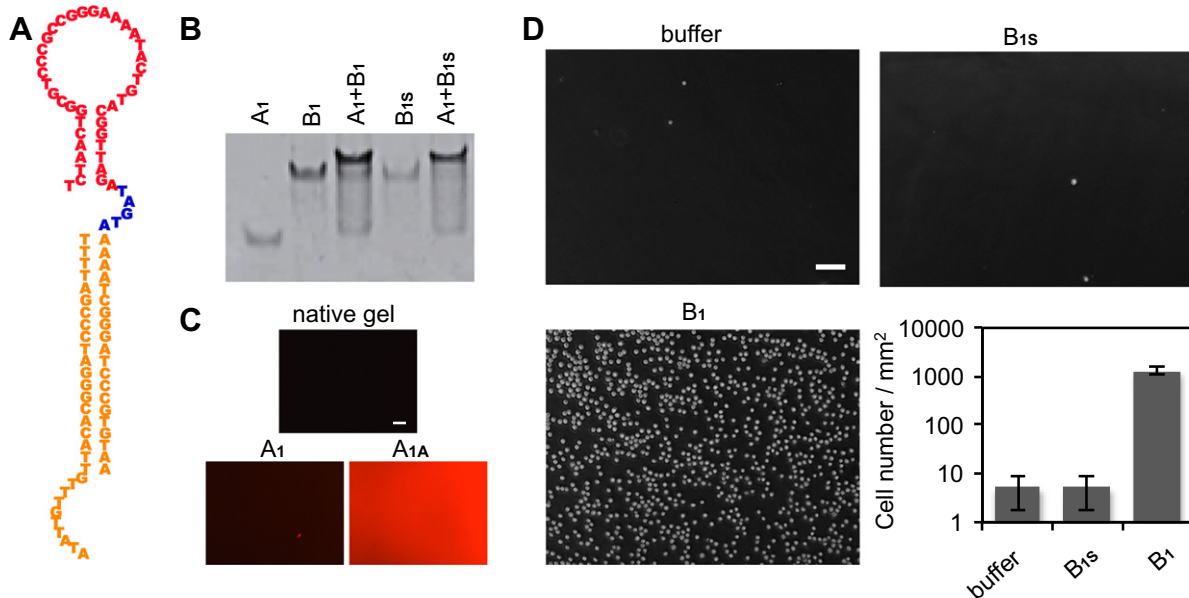


**Fig. 4.** Characterization of the functionality of the aptamer in catching CCRF-CEM cells. (A) Secondary structure of the hybridized aptamer. Red indicates the binding motif; blue indicates the linker and yellow indicates the hybridized segment. (B) Electrophoretogram of intermolecular hybridization. (C) Fluorescence images of hydrogel coatings treated with sequence  $B_{1T}$ . These hydrogels were thoroughly washed after  $B_{1T}$  treatment. Sequence  $B_{1T}$  carried TAMRA for clear legibility. Sequence  $A_1$  in the  $A_1$  hydrogel did not bear acrydite; sequence  $A_{1A}$  in the  $A_{1A}$  hydrogel was conjugated with acrydite. (D) Effect of different treatments on the capability of A-functionalized hydrogel in catching CCRF-CEM cells. Three A-functionalized hydrogel samples were treated with buffer,  $B_{1S}$ , and  $B_1$ , respectively. The cell images were captured under an inverted microscope. The cell numbers were quantified with ImageJ. Scale bar: 10  $\mu\text{m}$ . (For interpretation of the references to color in this figure legend, the reader is referred to the web version of this article.)

After the successful demonstration of intermolecular hybridization in the hydrogel, a cell catch experiment was run to examine whether the immobilized B<sub>1</sub> could induce cell binding to the hydrogel. The B<sub>1</sub> functionalized hydrogel could catch cells with the density over  $\sim 1000$  cells/mm<sup>2</sup> (Fig. 4D). In contrast, only  $\sim 10$  cells/mm<sup>2</sup> were observed on the other two control surfaces. These results demonstrate that the hybridized functional aptamers enabled the successful cell catch to the hydrogel coating.

The aptamer was purposely immobilized to the hydrogel using intermolecular hybridization rather than direct conjugation for an important concern. The aptamer is designed to carry an exogenous endonuclease-recognizing cleavage site comprised of nucleotides. These exogenous nucleotides may form intramolecular base pairs with the original nucleotides of the aptamer and therefore affect the binding affinity of the aptamer. The use of a hybridized aptamer can simply avoid this potential problem.

#### 3.4. Determination of cell type-specific catch

The success of cell catch relies on not only the ability to catch target cells, but also the ability to resist the binding of non-target cells. Therefore, another cell catch experiment was run to compare the binding of CCRF-CEM and Ramos (*i.e.*, control) cells. The flow cytometry analysis shows that the aptamer specifically binds to CCRF-CEM cells rather than Ramos cells (Fig. 5A). Consistent with the flow cytometry analysis, the aptamer was able to

catch CCRF-CEM cells rather than Ramos cells (Fig. 5B and C) to the hydrogel coating. The profile of binding kinetics shows that the density of Ramos cells on the hydrogel coating did not change throughout the experiment. Approximately 5 Ramos cells/mm<sup>2</sup> were observed on the hydrogel surface. In contrast, the cell density of CCRF-CEM cells rapidly increased during the first 30 min and then gradually reached plateau. These results show that the use of aptamers ensures cell type-specific catch to the hydrogel coating.

A number of other affinity ligands may also satisfy the need of cell type-specific catch. These ligands include but are not limited to antibodies, peptides, and certain small molecules (*e.g.*, folic acids). Although all of these affinity ligands can be in principle applied to catch target cells, we purposely used nucleic acid aptamers to catch cells for three main reasons. First, nucleic acid aptamers are synthetic oligonucleotides screened from DNA/RNA libraries with high binding affinities and specificities that are comparable to antibodies [37,38]. Second, aptamers are synthesized using standard phosphoramidite chemistry [39]. Thus, aptamers exhibit little or no batch-to-batch variation, which is definitely beneficial to increase the reliability of cell catch. Third, our ultimate goal is to achieve not only specific cell catch but also nondestructive cell release based on endonuclease-mediated cleavage. It is easy to design and synthesize nucleic acid aptamers with an endonuclease-recognizing site rather than DNA-antibody or DNA-peptide chimeras.

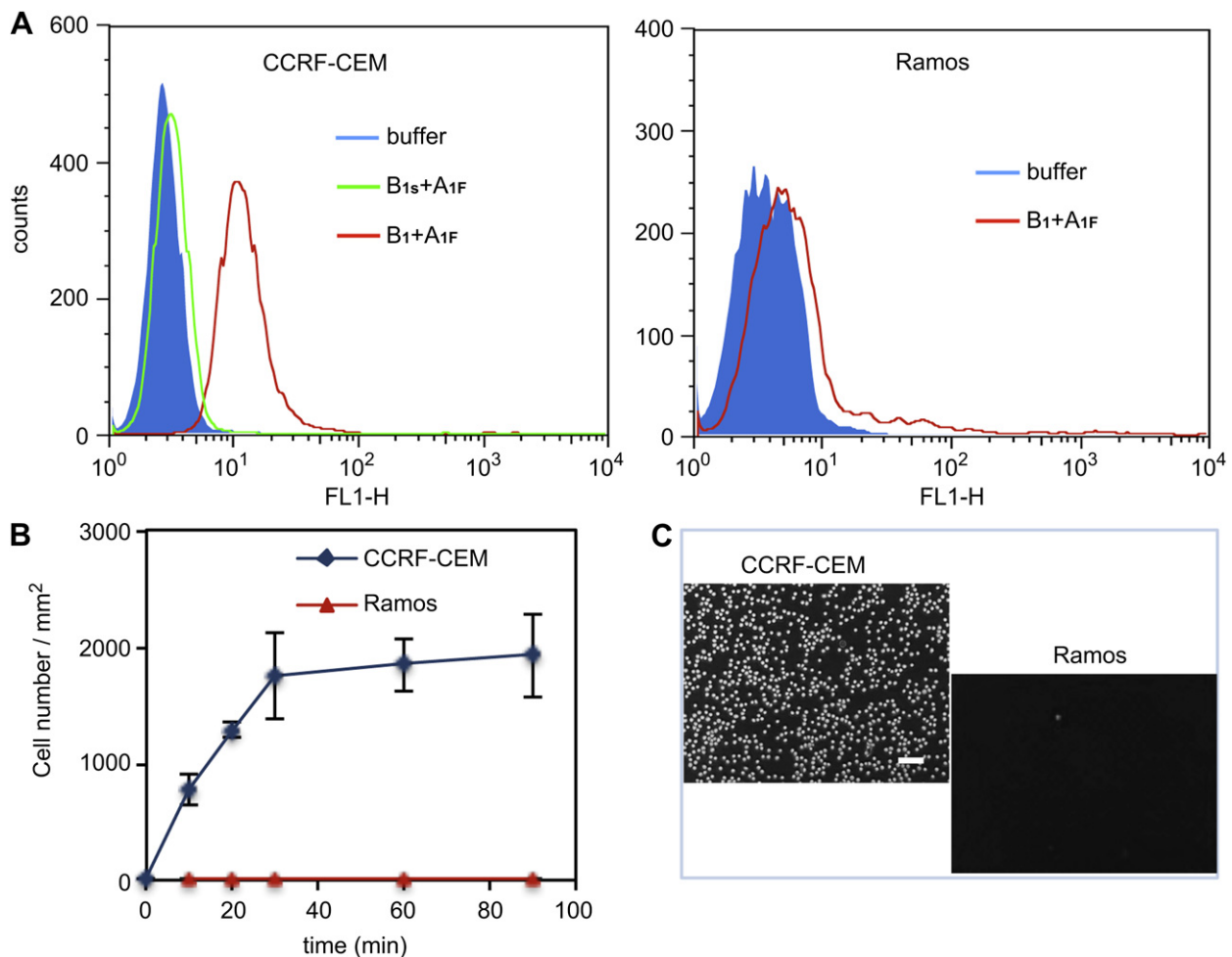


**Fig. 5.** Characterization of cell type-specific catch. (A) Flow cytometry histograms. (B) Kinetics of cell binding to the hydrogel coating. (C) Representative microscopy images of cells on the hydrogel coating. The images were captured at 30 min post cell seeding. Scale bar: 10  $\mu$ m.

### 3.5. Endonuclease-mediated sequence-specific hydrolysis for cell release

After cell catch and separation, it is also important to release cells with minimized cell damage for downstream cell characterization. To release the cells, we used a restriction endonuclease (*i.e.*, *Bam*HI) [40–42] to treat the aptamer-functionalized hydrogel coating. The cleavage sites of the aptamer duplex are shown in Fig. 6A. The gel electrophoretogram shows that the 30-min *Bam*HI treatment led to the degradation of the majority of  $A_1$ – $B_1$  duplexes (Fig. 6B). This result was confirmed by the flow cytometry analysis (Fig. 6C). After the demonstration of the effectiveness of using *Bam*HI to hydrolyze the  $A_1$ – $B_1$  duplexes, we performed a *Bam*HI-mediated cell release experiment. The cells and the hydrogel coatings were treated with *Bam*HI for 30 min. The result shows that the efficiency of cell release was ~99% and the cell density on the hydrogel coating was decreased to ~10 cells/mm<sup>2</sup> (Fig. 6D).

To confirm the observations in the *Bam*HI experiment and to illustrate the specificity of restriction endonucleases in releasing cells, we also examined the functionality of another restriction endonuclease, *i.e.*, *Kpn*I. The recognition sequences of *Bam*HI (Fig. 6A) and *Kpn*I (Fig. 7A) have a high similarity with only the middle two nucleotides switched to the corresponding positions. Despite the high similarity of their recognition sequences, these two endonucleases exhibited high fidelity and accuracy of cutting the recognition sequences (Fig. 7B). *Bam*HI hydrolyzed the  $A_1$ – $B_1$  duplex rather than the  $A_2$ – $B_2$  duplex; *Kpn*I hydrolyzed the  $A_2$ – $B_2$  duplex rather than the  $A_1$ – $B_1$  duplex. The cell release data are consistent with the gel electrophoresis results. For the hydrogels

functionalized with the  $A_1$ – $B_1$  duplex, the cells were released by *Bam*HI rather than *Kpn*I (Fig. 7C). For the hydrogel functionalized with the  $A_2$ – $B_2$  duplex, the cells were released by *Kpn*I rather than *Bam*HI (Fig. 7D). These results demonstrate that the restriction endonuclease-mediated cell release is sequence-specific.

Because tumor cells in the same tumor exhibit heterogeneous properties [43–45], it is reasonable that circulating tumor cells may have different characteristics. Thus, the ability to separate and detect the subgroups of circulating tumor cells may lead to a deep understanding of cancer development. In principle, multiple specific aptamers with different nuclease-recognizing sites can be rationally designed and immobilized into the hydrogel coating to catch the subgroups of tumor cells. Because our results have shown that *Bam*HI and *Kpn*I specifically hydrolyzed different recognition sequences (Fig. 7), it is promising that the subgroups of tumor cells would be specifically captured and released when sequence-specific aptamers and endonucleases were used.

### 3.6. Comparison of *Bam*HI and trypsin in releasing cells

In addition to restriction endonucleases, it is also possible to use proteases to induce cell release from the hydrogel coating. Thus, it is reasonable to question which type of enzyme will be more efficient to release cells from the hydrogel coating. To address this question, we compared the ability of *Bam*HI and trypsin in releasing cells. The reason for choosing trypsin for comparison is that trypsin is the most commonly used protease for detaching cells from a surface. As shown in Fig. 8A, *Bam*HI released  $95 \pm 4\%$  cells within 10 min whereas trypsin released  $80 \pm 18\%$  cells during the same

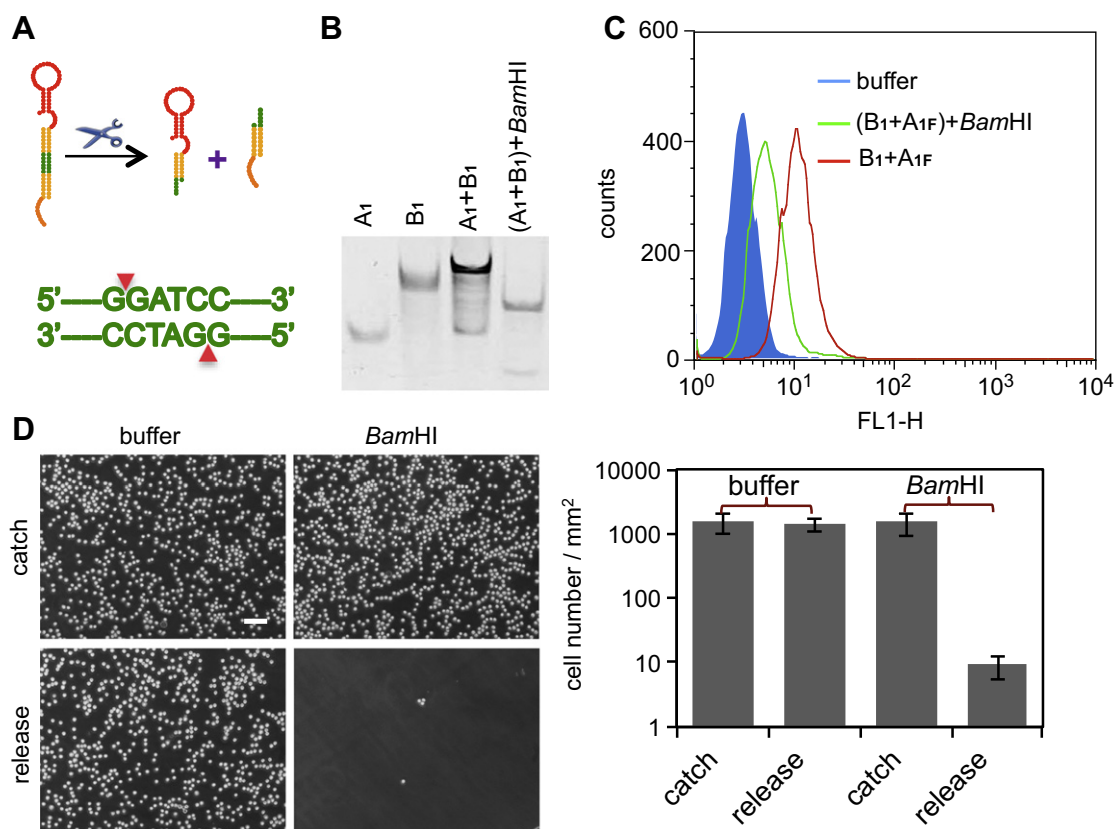


**Fig. 6.** *Bam*HI-mediated cell release from the hydrogel coating. (A) Schematic of *Bam*HI-mediated cleavage. The symbol of the scissor indicates the restriction endonuclease. The arrowheads point to the cleavage sites. (B) Gel electrophoretogram for analyzing the hydrolysis of the  $A_1$ – $B_1$  duplex. (C) Flow cytometry histogram for determining the binding capability of the hydrolyzed  $A_1$ – $B_1$  duplex.  $A_{1F}$ : sequence  $A_1$  labeled with FAM. (D) Microscopy images of cells on the hydrogel coating before and after *Bam*HI treatment. Scale bar: 10  $\mu$ m. The cell numbers were quantified using ImageJ.

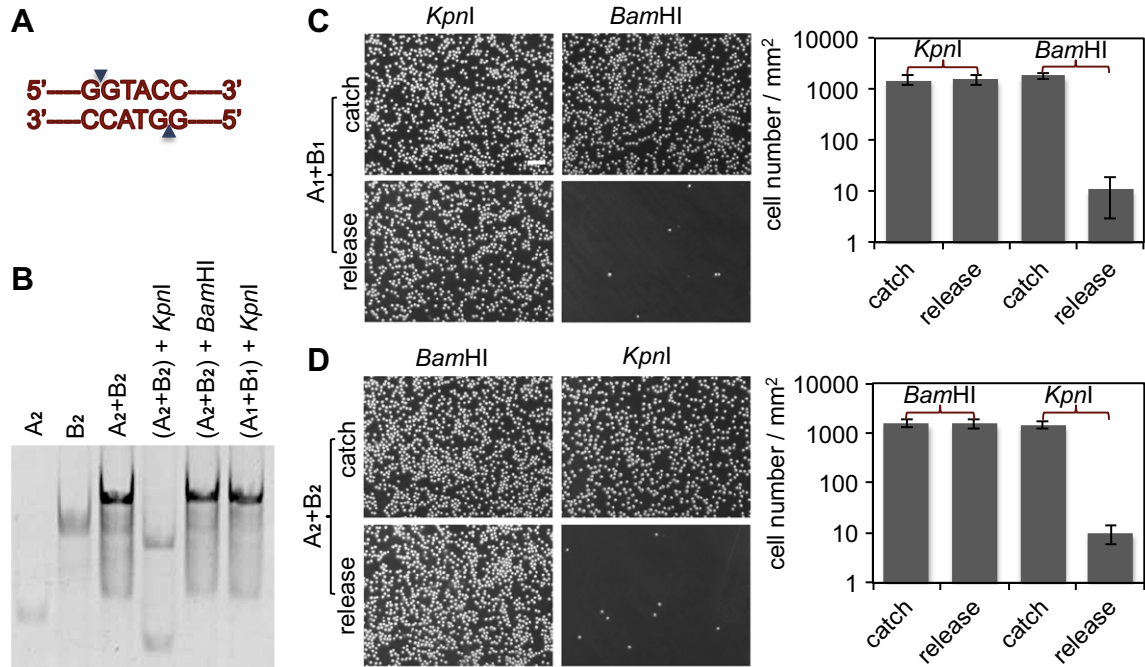


**Fig. 7.** Examination of sequence-specific DNA cleavage and cell release. (A) Recognition sequence of *KpnI*. The arrowheads point to the cleavage sites. (B) Gel electrophoretogram for analyzing the hydrolysis of the aptamer duplexes. (C&D) microscopy images of cells on the hydrogel coatings before and after endonuclease treatment. The hydrogel coatings were functionalized with A<sub>1</sub>–B<sub>1</sub> (C) and A<sub>2</sub>–B<sub>2</sub> duplexes (D). Scale bar: 10 μm. The cell images were analyzed using ImageJ to provide a quantitative analysis.

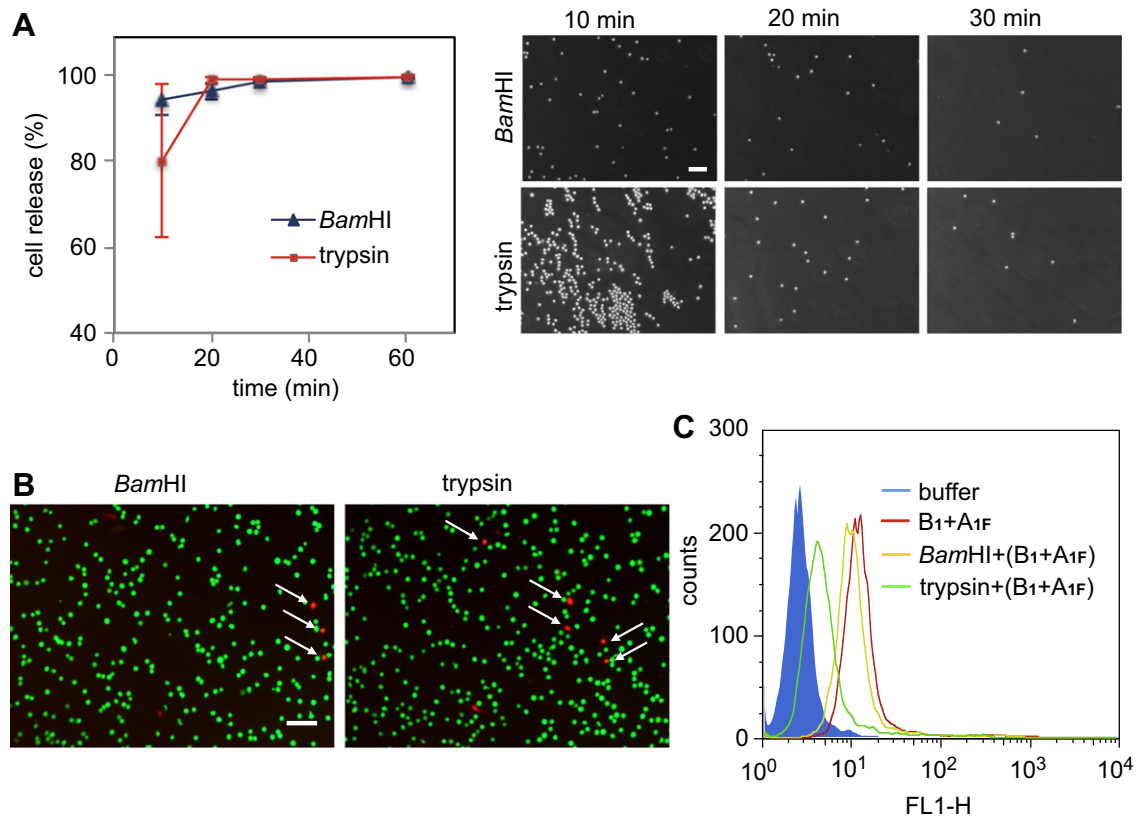


**Fig. 8.** Comparison of cell release mediated by *BamHI* and trypsin. (A) Cell release kinetics. (B) Live/dead cell staining. The green and red colors indicate live and dead (pointed by the arrows) cells, respectively. (C) Flow cytometry histogram for qualitatively analyzing the presence of cell receptors. Four groups of cells were compared, including cells treated with buffer, normal cells labeled with the B<sub>1</sub>–A<sub>1F</sub> duplex, cells released by *BamHI* and labeled with the B<sub>1</sub>–A<sub>1F</sub> duplex, and cells released by trypsin and labeled with the B<sub>1</sub>–A<sub>1F</sub> duplex. Scale bar: 10 μm. (For interpretation of the references to color in this figure legend, the reader is referred to the web version of this article.)



period of time. In addition, the unreleased cells in the trypsin group were not evenly distributed on the hydrogel coating. These differences may be partly attributed to the steric hindrance. Cell receptors are directly attached to a compact cell membrane whereas the aptamers are immobilized on the porous hydrogel coating. In addition, the cleavage sites of endonucleases are located in the middle of double-stranded helices. Resultantly, it would be easier for endonucleases to attack the cleavage sites than proteases to attack cell receptors. The results also show that both trypsin and *Bam*HI could release more than 99% cells after 30-min enzyme treatment (Fig. 8A).

Because the analysis of circulating tumor cells involve the characterization of not only signaling molecules and genes inside the cells but also their surface properties, it is critical to ensure minimal effects on cell properties both inside and on the surface during the procedure of cell release. This need is particularly important to the understanding of the properties of metastatic cancer cells that may rely on their surface receptors to find appropriate places to survive and grow into new tumors. Therefore, in addition to the cell release efficiency, we further compared the properties of released cells with two different assays: Live/dead cell staining and flow cytometry. The results show that the percentage of viable cells was approximately 98% in both groups, indicating that there is no difference between *Bam*HI and trypsin in affecting cell viability (Fig. 8B). However, the flow cytometry results show a significant difference (Fig. 8C). The *Bam*HI-released cells exhibited fluorescence intensity similar to that of normal cells whereas the trypsin-released ones exhibited fluorescence intensity close to that of the unlabeled cells. These results demonstrate that endonucleases barely affect cell receptors whereas proteinases cause a significant decrease of receptor density. Taken together, these cell release results indicate that endonuclease-mediated treatment is not only fast and efficient, but also nondestructive to cells.

#### 4. Conclusions

A material system for cell catch and release was developed using aptamer-functionalized hydrogels and restriction endonucleases. The immobilized aptamers can specifically catch target cancer cells on the hydrogel surface that is highly resistant to nonspecific cell binding. In addition, sequence-specific restriction endonucleases can hydrolyze aptamers with rationally designed cleavage sites and rapidly release cells from the hydrogel without causing cell damage. Therefore, aptamer-functionalized hydrogels hold great potential as a coating material to functionalize medical devices (e.g., microfluidic devices) for specific catch and nondestructive release of rare circulating tumor cells.

#### Acknowledgments

We thank Dr. Carol Norris and Mr. Liang Su for technical support. The support from the US National Science Foundation (CBET-1033212) is also greatly acknowledged. S.L. and N.C. were supported in part by the China Scholarship Council.

#### References

- [1] Webster DR, Sabbadini E. The prognostic significance of circulating tumour cells: a five-year follow-up study of patients with cancer of the breast. *Can Med Assoc J* 1967;96:129–31.
- [2] Engel H, Kleespies C, Friedrich J, Breidenbach M, Kallenborn A, Schöndorf T, et al. Detection of circulating tumour cells in patients with breast or ovarian cancer by molecular cytogenetics. *Br J Cancer* 1999;81:1165–73.
- [3] Ring A, Smith IE, Dowsett M. Circulating tumour cells in breast cancer. *Lancet Oncol* 2004;5:79–88.

- [4] Hogan BV, Peter MB, Shenoy H, Horgan K, Hughes TA. Circulating tumour cells in breast cancer: prognostic indicators, metastatic intermediates, or irrelevant bystanders? [Review]. *Mol Med Rep* 2008;1:775–9.
- [5] Krell J, Stebbing J. Circulating tumour cells as biomarkers in early breast cancer. *Lancet Oncol* 2012;13:653–4.
- [6] Goeminne JC, Guillaume T, Salmon M, Machiels JP, D'Hondt V, Symann M. Unreliability of carcinoembryonic antigen (CEA) reverse transcriptase-polymerase chain reaction (RT-PCR) in detecting contaminating breast cancer cells in peripheral blood stem cells due to induction of CEA by growth factors. *Bone Marrow Transplant* 1999;24:769–75.
- [7] Jung R, Krüger W, Hosch S, Holweg M, Kröger N, Gutensohn K, et al. Specificity of reverse transcriptase polymerase chain reaction assays designed for the detection of circulating cancer cells is influenced by cytokines in vivo and in vitro. *Br J Cancer* 1998;78:1194–8.
- [8] Brossart P, Schmier JW, Krüger S, Willhauck M, Scheibenbogen C, Monier T, et al. A polymerase chain reaction-based semiquantitative assessment of malignant melanoma cells in peripheral blood. *Cancer Res* 1995;55:4065–8.
- [9] Sabbatini R, Federico M, Morselli M, Depenni R, Cagossi K, Luppi M, et al. Detection of circulating tumor cells by reverse transcriptase polymerase chain reaction of mspin in patients with breast cancer undergoing conventional-dose chemotherapy. *J Clin Oncol* 2000;18:1914–20.
- [10] Osborne MP, Asina S, Wong GY, Old LJ, Cote RJ. Immunofluorescent monoclonal antibody detection of breast cancer in bone marrow: sensitivity in a model system. *Cancer Res* 1989;49:2510–3.
- [11] Gross HJ, Verwer B, Houck D, Recktenwald D. Detection of rare cells at a frequency of one per million by flow-cytometry. *Cytometry* 1993;14:519–26.
- [12] Brown M, Wittwer C. Flow cytometry: principles and clinical applications in hematology. *Clin Chem* 2000;46:1221–9.
- [13] Nagrath S, Sequist LV, Maheswaran S, Bell DW, Irimia D, Utkus L, et al. Isolation of rare circulating tumour cells in cancer patients by microchip technology. *Nature* 2007;450:1235–9.
- [14] Adams AA, Okagbare PI, Feng J, Hupert ML, Patterson D, Göttert J, et al. Highly efficient circulating tumor cell isolation from whole blood and label-free enumeration using polymer-based microfluidics with an integrated conductivity sensor. *J Am Chem Soc* 2008;130:8633–41.
- [15] Mayumi M, Sumimoto SI, Kanazashi SI, Hata D, Yamaoka K, Higaki Y, et al. Negative signaling in B cells by surface immunoglobulins. *J Allergy Clin Immunol* 1996;98:S238–47.
- [16] Smith JA, Bluestone JA. T cell inactivation and cytokine deviation promoted by anti-CD3 mAbs. *Curr Opin Immunol* 1997;9:648–54.
- [17] Henke C, Bitterman P, Roongta U, Ingbar D, Polunovsky V. Induction of fibroblast apoptosis by anti-CD44 antibody: implications for the treatment of fibroproliferative lung disease. *Am J Pathol* 1996;149:1639–50.
- [18] El-Ali J, Sorger PK, Jensen KF. Cells on chips. *Nature* 2006;442:403–11.
- [19] Reisewitz S, Schroeder H, Tort N, Edwards KA, Baesumner AJ, Niemeyer CM. Capture and culturing of living cells on microstructured DNA substrates. *Biomed Mater* 2010;6:2162–8.
- [20] Phillips JA, Xu Y, Xia Z, Fan ZH, Tan WH. Enrichment of cancer cells using aptamers immobilized on a microfluidic channel. *Anal Chem* 2009;81:1033–9.
- [21] Wan Y, Kim Y, Li N, Cho SK, Bachoo R, Ellington AD, et al. Surface-immobilized aptamers for cancer cell isolation and microscopic cytology. *Cancer Res* 2010;70:9371–80.
- [22] Chen L, Liu X, Su B, Li J, Jlang L, Hang D, et al. Aptamer-mediated efficient capture and release of T lymphocytes on nanostructured surfaces. *Adv Mater* 2011;23:4376–80.
- [23] Plouffe BD, Brown MA, Iyer RK, Radisic M, Murthy SK. Controlled capture and release of cardiac fibroblasts using peptide-functionalized alginate gels in microfluidic channels. *Lab Chip* 2009;9:1507–10.
- [24] Soontornworajit B, Zhou J, Shaw MT, Fan TH, Wang Y. Hydrogel functionalization with DNA aptamers for sustained PDGF-BB release. *Chem Commun* 2010;46:1857–9.
- [25] Chen N, Zhang Z, Soontornworajit B, Zhou J, Wang Y. Cell adhesion on an artificial extracellular matrix using aptamer-functionalized PEG hydrogels. *Biomaterials* 2012;33:1353–62.
- [26] Zhu Z, Wu C, Liu H, Zou Y, Zhang X, Kang H, et al. An aptamer cross-linked hydrogel as a colorimetric platform for visual detection. *Angew Chem Int Ed* 2010;49:1052–6.
- [27] Banerjee I, Pangule RC, Kane RS. Antifouling coatings: recent developments in the design of surfaces that prevent fouling by proteins, bacteria, and marine organisms. *Adv Mater* 2011;23:690–718.
- [28] Harbers GM, Emoto K, Greef C, Metzger SW, Woodward HN, Mascali JJ, et al. Functionalized poly(ethylene glycol)-based bioassay surface chemistry that facilitates bio-immobilization and inhibits nonspecific protein, bacterial, and mammalian cell adhesion. *Chem Mater* 2007;19:4405–14.
- [29] Yang CY, Huang LY, Shen TL, Yeh JA. Cell adhesion, morphology and biochemistry on nano-topographic oxidized silicon surfaces. *Eur Cells Mater* 2010;20:415–30.
- [30] Kairdolf BA, Mancini MC, Smith AM, Nie SM. Minimizing nonspecific cellular binding of quantum dots with hydroxyl-derivatized surface coatings. *Anal Chem* 2008;80:3029–34.
- [31] Lee MH, Brass DA, Morris R, Composto RJ, Ducheyne P. The effect of non-specific interactions on cellular adhesion using model surfaces. *Biomaterials* 2005;26:1721–30.
- [32] Uchida K, Otsuka H, Kaneko M, Kataoka K, Nagasaki Y. A reactive poly(ethylene glycol) layer to achieve specific surface plasmon resonance sensing with a high

- S/N ratio: the substantial role of a short underbrushed PEG layer in minimizing nonspecific adsorption. *Anal Chem* 2005;77:1075–80.
- [33] Senaratne W, Andruzzi L, Ober CK. Self-assembled monolayers and polymer brushes in biotechnology: current applications and future perspectives. *Biomacromolecules* 2005;6:2427–48.
- [34] Cho WK, Kong B, Choi IS. Highly efficient non-biofouling coating of zwitterionic polymers: poly((3-(methacryloylamino)propyl)-dimethyl(3-sulfopropyl) ammonium hydroxide). *Langmuir* 2007;23:5678–82.
- [35] Jiang S, Cao Z. Ultralow-fouling, functionalizable, and hydrolyzable zwitterionic materials and their derivatives for biological applications. *Adv Mater* 2009;22:920–32.
- [36] Shangguan D, Li Y, Tang Z, Cao ZC, Chen HW, Mallikaratchy P, et al. Aptamers evolved from live cells as effective molecular probes for cancer study. *Proc Natl Acad Sci U S A* 2006;103:11838–43.
- [37] Ellington AD, Szostak JW. In vitro selection of RNA molecules that bind specific ligands. *Nature* 1990;346:818–22.
- [38] Tuerk C, Gold L. Systematic evolution of ligands by exponential enrichment: RNA ligands to bacteriophage T4 DNA polymerase. *Science* 1990;249:505–10.
- [39] Jayasena SD. Aptamers: an emerging class of molecules that rival antibodies in diagnostics. *Clin Chem* 1999;45:1628–50.
- [40] Hinsch B, Kula MR. Physical and kinetic-properties of the site specific endonuclease BamHI from *Bacillus amyloliquefaciens*. *Nucleic Acids Res* 1980;8:623–33.
- [41] Pingoud A, Jeltsch A. Recognition and cleavage of DNA by type-II restriction endonucleases. *Eur J Biochem* 1997;246:1–22.
- [42] Venkatesh S, Wower J, Byrne ME. Nucleic acid therapeutic carriers with on-demand triggered release. *Bioconjug Chem* 2009;20:1773–82.
- [43] Dexter DL, Kowalski HM, Blazar BA, Fligiel Z, Vogel R, Heppner GH. Heterogeneity of tumor-cells from a single mouse mammary tumor. *Cancer Res* 1978;38:3174–81.
- [44] Fargion S, Carney D, Mulshine J, Rosen S, Bunn P, Jewett P, et al. Heterogeneity of cell surface antigen expression of human small cell lung cancer detected by monoclonal antibodies. *Cancer Res* 1986;46:2633–8.
- [45] Poste G, Tzeng J, Doll J, Breig R, Rieman D, Zeidman I. Evolution of tumor cell heterogeneity during progressive growth of individual lung metastases. *Proc Natl Acad Sci U S A* 1982;79:6574–8.